substance: boron compounds with group II elements
property: properties of boron-alkaline earth compounds

Alkaline earth hexaborides CaB_6, SrB_6, BaB_6

Structure

The CaB_6-type lattice structure, the same for all alkaline earth hexaborides, is characterized by a three-dimensional skeleton of B_6 octahedra, whose interstices are occupied by metal atoms. Hence the crystal has cubic symmetry [66N, 69E, 60M, 75S, 77E]. The covalent boron sublattice is electron deficient and an electron transfer of at least one per atom from the metal sublattice to that of boron is required for stabilization [66N, 54B, 54E, 60L, 77E, 77P, 79A2, 77S2].

space group: O_h^1 – Pm3m.

lattice structure: Fig. 1

For linear thermal expansion, see below.

electron density contours: Fig. 2

ESCA spectrum: Fig. 3

Brillouin zone: Fig. 4

CaB_6

lattice parameter

a	4.1520 Å	T = 300 K	X-ray diffraction	70E2, 77E
	4.148 Å			75S

X-ray diffraction of CaB_6 compared with LaB_6, YbB_6 and ThB_6 in [82B].

Multipole deformation densities through the B_4 square of the octahedron in Fig. 5 [94I1], on the triangular face of the octahedron in Fig. 6 [94I1]. For previous, somewhat different results of the same authors, see [90I].

Radial distribution of the total electrons around the Ca atom in Fig. 7 [94I2]. For previous, somewhat different results of the same authors, see [90I].

band structure and density of states: Fig. 8. Somewhat different results in [77P and 86B].

Qualitatively different result of band structure calculation in [97M] indicating semimetallic instead of semiconducting properties.

energy gap

E_g	2.11 eV		calculated	77P
	0.3 eV		calculated (see Fig. 8)	79H
	0.4 eV	T > 820 K	electrical resistance	63J
	0.2 eV	T > 500 K	electrical conductivity	70P

For vibrational frequencies [88T, 90Y, 93Y].

IR diffuse reflectance spectra of CaB_6 in Fig. 9 [88T, 93Y].

Force constants [90Y].

Raman spectrum of CaB_6 in Fig. 10 [88T].

Irradiation-induced damage rates in [95C].

Entropy in [86B].

resistivity

ρ	0.1 Ω cm	T = 300 K	polycrystal	63J
	0.43 Ω cm	T = 300 K		70P
	0.16 Ω cm	T = 600 K		

density

d	2.45 g cm^{-3}		calculated	75S

	2.49 g cm^{-3}		experimental	

melting point

T_m	2230°C			74S
	2235°C			51L

coefficient of linear thermal expansion

α_{av}	$5.64 \cdot 10^{-6}$ K^{-1}			75S

Thermal expansion coefficient: α [10^{-6}K^{-1}] = 4.1510 (1+$5.64 \cdot 10^{-6}$ T + $1.74 \cdot 10^{-9} T^2$), T in K [73D].

SrB_6

lattice parameter

a	4.1981 Å	T = 300 K	X-ray diffraction	70E2, 77E
	4.190 Å			75S

Force constants [90Y].

ESR study of $EuB_{6-x}C_x$ including the comparison with some corresponding $YbB_{6-x}C_x$, $SrB_{6-x}C_x$, $Eu_{1-x}Gd_xB_6$, $Eu_{1-x}Sr_xB_6$ and $Eu_{1-x}La_xB_6$ compounds in [81T].

Calculation of the electronic band structure indicating semimetallic behavior in Fig. 11 [97M].

Density of electronic states calculation in Fig. 12 [97M].

energy gap

E_g	3.68 eV		ca]culated	77P
	0.38 eV	T > 1250 K	electrical resistance	63J
	0.45 eV	T > 700 K		60E
	12 meV	T = 7.2 ··· 46 K	electron-tunneling	98A

SrB_6 does not possess f bands and is nonmagnetic in contrast to SmB_6, EuB_6 and CeB_6 [98A].

For vibrational frequencies [88T, 90Y, 93Y].

Variation of Raman spectra depending on the change in particles in Fig. 13 [93Y].

IR diffuse reflectance spectra of SrB_6 in Fig. 9 [93Y].

Raman spectrum of SrB_6 in Fig. 10 [88T, 93Y].

Comparison between IR transmittance and photoacoustic spectrum in [88T].

resistivity

ρ	0.216 Ω cm	T = 300 K	singlecrystal	63J

density

d	3.42 g cm^{-3}		calculated	75S
	3.28 g cm^{-3}		experimental	

melting point

T_m	2235°C			51L

coefficient of linear thermal expansion

α_{av}	$6.7 \cdot 10^{-6}$ K^{-1}			75S

work function

SrB_6

Φ	4.24...4.38 eV	A = 29...120 A cm^{-2} K^{-2}	A: emission constant, defined by $i_s = AT^2 \exp(-\Phi/kT)$ where i_s is the saturation current density	78R

Entropy in [86B].

BaB_6

lattice parameter

a	4.2706 Å	T = 300 K	X-ray diffraction	61J, 77E
	4.280 Å			75S

Preparation of BaB_6 powders and thermionic emission characteristics in [79A1].

energy gap

E_g	2.64 eV		calculated	77P
	0.12 eV	T > 700 K	electrical resistance	63J
	0.15 eV	T > 300 K	electrical conductivity	70P

resistivity

ρ	0.07 Ω cm	T = 300 K		70P
	0.01 Ω cm	T = 600 K		

For resistivity, see also [75S].

density

d	4.25 g cm^{-3}		calculated	75S
	4.26 g cm^{-3}		experimental	

melting point

T_m	2270°C			51L

coefficient of linear thermal expansion

α_{av}	$6.8 \cdot 10^{-6}$ K^{-1}			75S

Entropy in [86B].

Ternary compounds

System CaB_6–SmB_6: see [79S; 77S2; 79R].

References:

51L Lafferty, J.: J. Appl. Phys. 22 (1951) 299.

54B Blum, P., Bertraut, F.: Acta Crystallogr. 7 (1954) 81.

54E Eberhardt, W. H., Crawford, J. B., Lipscomb, W. N.: J. Chem. Phys. 22 (1954) 989.

59S Samsonov, G.V., Shravlev, N.N., Paderno, Yu.B., Melik-Adamyai, V.R.: Kristallografiya 4 (1959) 538 (in Russian).

60B Binder, I., La Placa, S., Post, B., in: Boron I, J. A. Kohn, W. F. Nye, G. K. Gauld, eds., Plenum Press: New York, 1960 p. 86.

60E Eubank, W. R., Pruitt, L. E., Thurnaner, H.: see [60B], p. 116.

60G Giardini, A. A., Kohn, J. A., Toman, L., Eckart, D. W.: see [60E], p. 140.

60L Lipscomb, W. N., Britton, D.: J. Chem. Phys. 33 (1960) 275.

60M McDonald, B. J., Stuart, W. I.: Acta Crystallogr. 13 (1960) 447.

61J Johnson, R. W., Daane, A. H.: J. Phys. Chem. 65 (1961) 909.

63J Johnson, R. W., Daane, H. H.: J. Chem. Phys. 38 (1963) 425.

66N Naslain, R., Etourneau, J.: C. R. Acad. Sci. (Paris) 263 (1966) 484.

69E Eick, H. A., Mulford, R. N. R.:J. Inorg. Nucl. Chem. 31 (1969) 371.

70E1 Boron 3, T. Niemyski, ed., PWN Warsaw, 1970

70E2 Etourneau, J., Thèse de Doct. Sci. Phys. Univ. Bordeaux I, 1970.

70P Paderno, Yu. B., Goryachev, Yu. M., Garf, E. S.: see [70E1] p. 175.

73D Dudchak, Ya.I., Fedishin, Ya.I., Paderno, Yu.B., Vadez, D.I.: Izv. Akad. Nauk. SSSR Ser. Fiz. 1 (1973) 154 (in Russian).

74K Korsukova, M. M., Gurin, V. N., Sorokin, V. N., Yusov, Yu. P., Terent'eva, S. P., in: Bor, Poluchenie, Struktura i Svoistva, Ed.: Tavadze F. N., Moscow Nauka, 1974, p. 235.

74S Samsonov, G. V., Goryachev, Yu. M., Kovenskaya, B. A., Arabej, B. C.: see [74K], p. 171.

75S Samsonov, G. V., Serebryakova, T. I., Neronov, V. A.: Boridy, Moskva Atomizdat, 1975.

76A Aono, M., Kawai, S., Kono, S., Okusawa, M., Sagawa, T., Takehana, Y.: J. Phys. Chem. Solids37 (1976) 215.

77B Berezin, A. A., Golikova, O. A., Zaitsev, V. R., Kazanin, M. M., Orlov, V. M., Tkalenko, E. N., in:Boron and Refractory Borides, (Matkovich V. 1., ed.) Springer: Berlin, Heidelberg, New York 1977, p. 52.

77E Etourneau, J., Mercuno, J. P., Hagenmuler, P.: see [77B], p. 115.

77P Perkins, P. G.: see [77B], p. 31.

77S1 Samsonov, G. V., Kovenskaya, B. A.: see [77B], p. 5.

77S2 Samsonov, G. V., Rud', B. M., Shulishova, O. I., Konovalova, F. S., Mudrolyubov, Yu. M., Budanova, I. G.: Izd. Akad. Nauk SSSR Neorg. Mater. 13 (1977) 1314.

78R Report Nat. Inst. Research in Inorg. Mater. 17 (1978) 44.

79A1 Abrahams, E., Anderson, P.W., Licciardelle, D.C., Ramakrishnan, T.V: Phys. Rev. Lett. 42 (1979) 673.

79A2 Aleshin, V. G., Kosolapova, T. Ya., Nemoshkalenko, V. V., Serebryakova, T. I., Chudimov, N. G.: J. Less Common Met. 67 (1979) mr

79H Hasegawa, A., Yanase, A.: J. Phys. C 12 (1979) 5431.

79R Rud', B. M., Levandovskii, V. D., Skulishova, O. I.: Izv. Akad. Nauk, Neorg. Mater. 15 (1979) 709; Inorg. Mater. (English Transl.) 15 (1979) 553.

79S Rud', B. M., Levandovskii, V. D., Shulishova, O. I.: Izv. Akad. Nauk SSSR Neorg. Mater. 15 (1979) 709.

81S Shelykh, A.I., Sidorin, K.K., Karin, M.G., Bobrikov, V.N., Korsukova, M.M., Gurin, V.N., Smirnov, I.A.: J. Less-Common Met. 82 (1981) 291.

81T Tarascon, J.M., Etourneau, J., Dance, J.M., Hagenmuller, P., Georges, R., Angelov, S., v. Molnar, S.: J. Less-Common Met. 82 (1981) 277 (Proc. 7th Int. Symp. Boron, Borides and Rel. Compounds, Uppsala, Sweden, 1981).

82B Barantseva, I.G., Paderno, Yu.B.: Sov. Powder Metall. Met. Ceram. 21 (1982) 585.

86B Bullett, D.W.: in: Boron-Rich Solids (AIP Conf. Proc. 140), Albuquerque, New Mexico 1985, D. Emin, T.L. Aselage, C.L. Beckel, I.A. Howard ed., American Institute of Physics: New York, 1986, p. 249.
86B Borovikova, M.S., Fesenko, V.V.: J. Less-Common Met. 117 (1986) 287. (Proc. 8th Int. Symp. Boron, Borides, Carbides, Nitrides and Rel. Compounds, Tbilisi, Oct. 8 - 12, 1984)
88T Turrell, S., Yahia, Z., Huvenne, J.P., Lacroix, B., Turrell, G.: J. Mol. Struct. 174 (1988) 455.
90I Ito, T., Higashi, I.: in: Proc. 12th Seminar on Science and Technology "Crystallography", Tokyo, 5 - 6 March 1990, Interchange Association, Japan: Tokyo, 1990, p. 53.
90Y Yahia, Z., Turrell, S., Turrell, G., Mercurio, J.P.: J. Mol. Struct. 224 (1990) 303.
93Y Yahia, Z., Turrel, S., Mercurio, J.P., Turrel, G.: J. Raman Spectroscopy 24 (1993) 207.
94I1 Ito, T., Kasukawa, T., Higashi, I., Satow, Y.: Proc. 11th Int. Symp. Boron, Borides and Rel. Compounds, Tsukuba, Japan, August 22 - 26, 1993, Jpn. J. Appl. Phys. Series 10 (1994), p. 11.
94I2 Izumi, K., Yoshikawa, N., Kudaka, K., Okada, S., Lundström, T.: Proc. 11th Int. Symp. Boron, Borides and Rel. Compounds, Tsukuba, Japan, August 22 - 26, 1993, Jpn. J. Appl. Phys. Series 10 (1994), p. 156.
95C Carrard, M., Emin, D., Zuppiroli, L.: Phys. Rev. B 51 (1995) 11270.
97M Massidda, S., Continenza, A., de Pascale, T.M., Monnier, R.: Z. Phys. B. 102 (1997) 83.
98A Ambler, B., Fisk, Z., Sarrao, J.L., v. Molnar, S., Meisel, M.W., Sharifi, F.: Phys. Rev. B 57 (1998) 8747.
99W Werheit, H., Au, T., Schmechel, R., Paderno, Yu.B., Konovalova, E.S.: J. Solid State Chem. (2000) (Proc. 13th Int. Symp. Boron, Borides and Rel. Compounds, Dinard, France, Sept. 1999).

Fig. 1.

CaB_6. Lattice structure [77E].

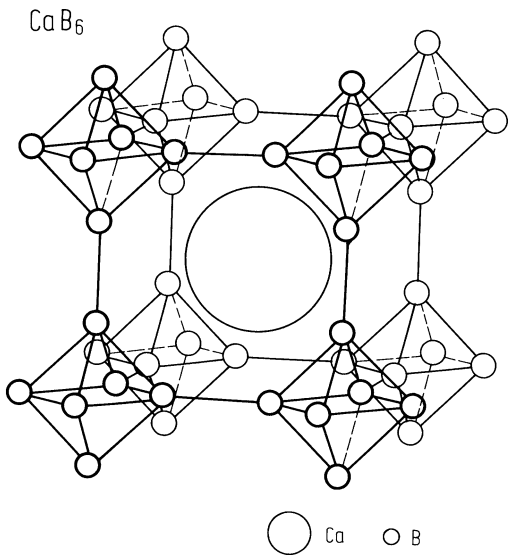

Fig. 2.

CaB_6. (a) Electron density contour across the fourfold axis of the octahedron. (b) Electron density contour across theeight trigonal faces of B_6^{2-} cage [77P]. Electron density in e $Å^{-3}$.

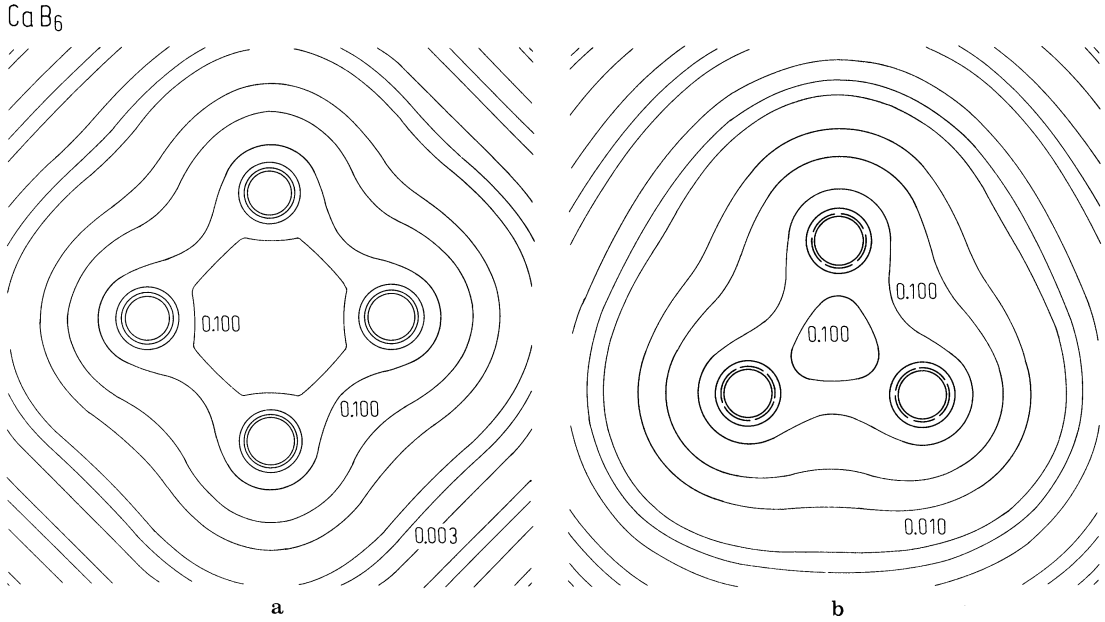

Fig. 3.

CaB_6. The ESCA spectrum of CaB_6 including the energy band region. The charging-up effect has been corrected for and hence the position $E_b^F = 0$ coincides with the Fermi level within experimental error (10.2 eV). The dotted curves denote the $\alpha_{3,4}$ satellite peaks of the Ca 3s and 3p main peaks [76A].

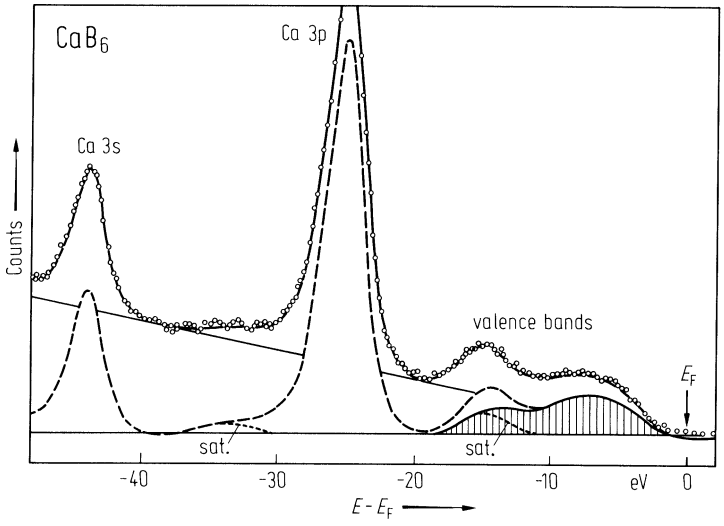

Fig. 4.

CaB_6. Brillouin zone for the cubic reciprocal lattice [77P].

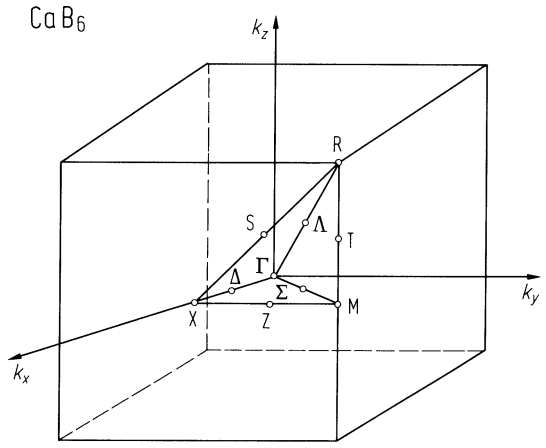

Fig. 5.

CaB_6. Multipole deformation densities at z = ½, through the B_4 square of the octahedron. Contours at 0.05 eÅ^{-3}, negative contours dotted [94I1].

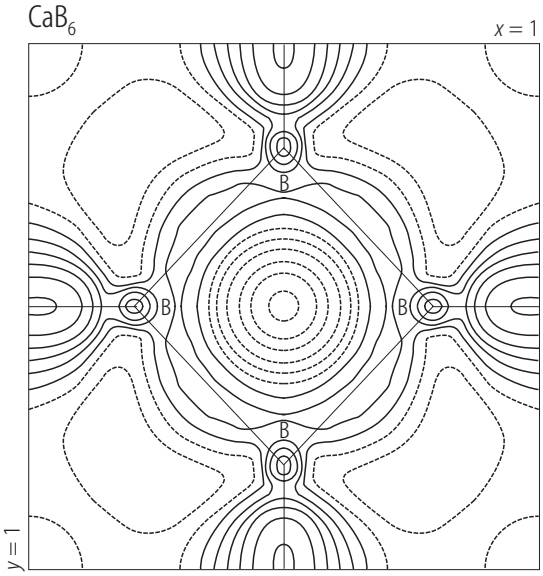

Fig. 6.

CaB_6. Multipole deformation densities on the triangular face of the octahedron. Contours at 0.05 $eÅ^{-3}$, negative contours dotted [94I1].

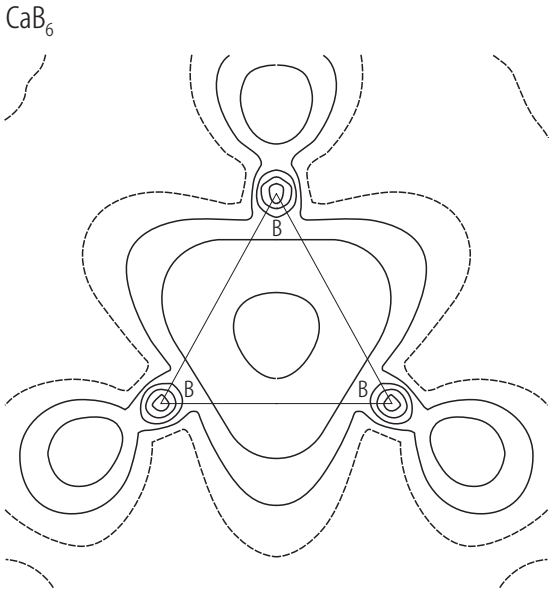

Fig. 7.

CaB_6. Radial electron density distribution around Ca. Solid line, observed; dotted line, theoretical calculation for a Ca^{2+} ion [94I1].

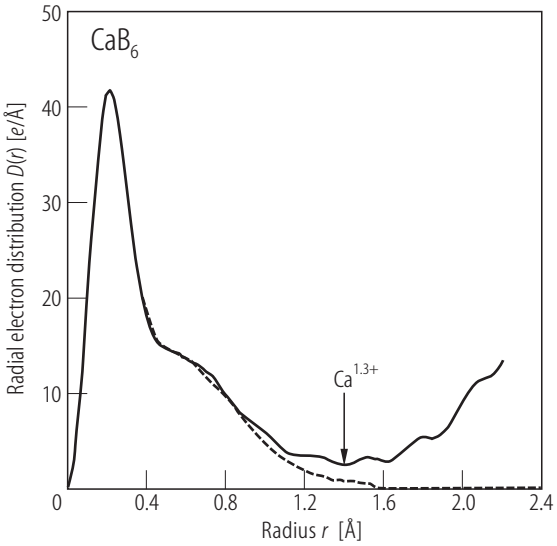

Fig. 8.

CaB_6. Self consistent APW energy band structure and density of states, calculated with the local-spin-density approximation and with the non-muffin-tin corrections. The symmetry labels denote irreducible representations about the center of the B_6 octahedron. The two broken lines show the energy gap between the valence and conduction bands. The DOS is the total DOS for the lowest 13 bands [79H].

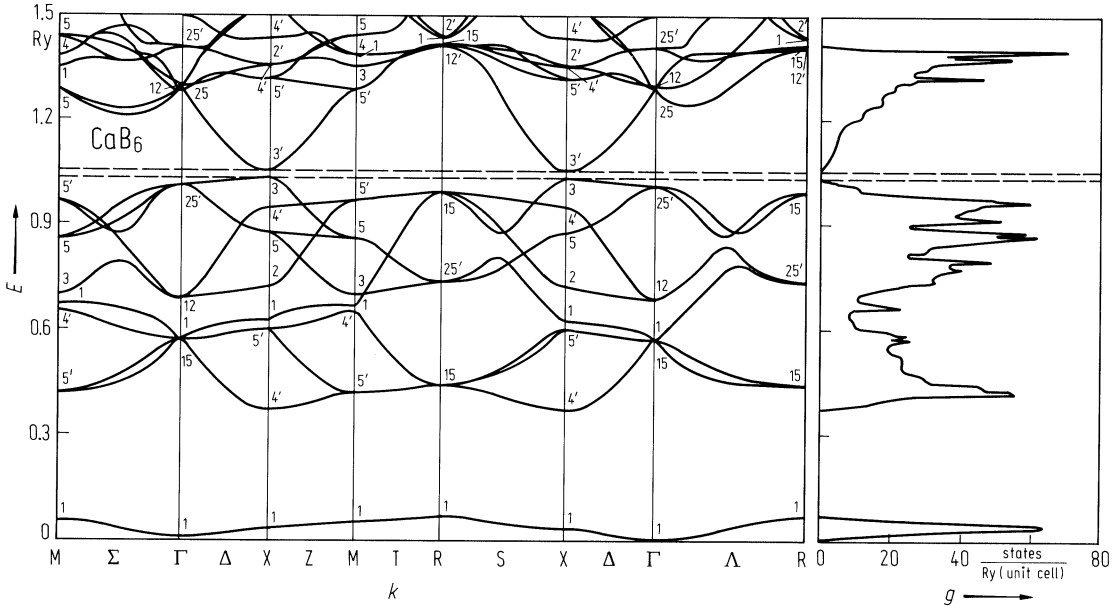

Fig. 9.

Metal hexaborides. IR diffuse reflectance spectra of representative MB_6 compounds with two-valent Ca, Sr and Yb, and three-valent Nd, Gd, La, Tb and Dy metal atoms [88T, 93Y].

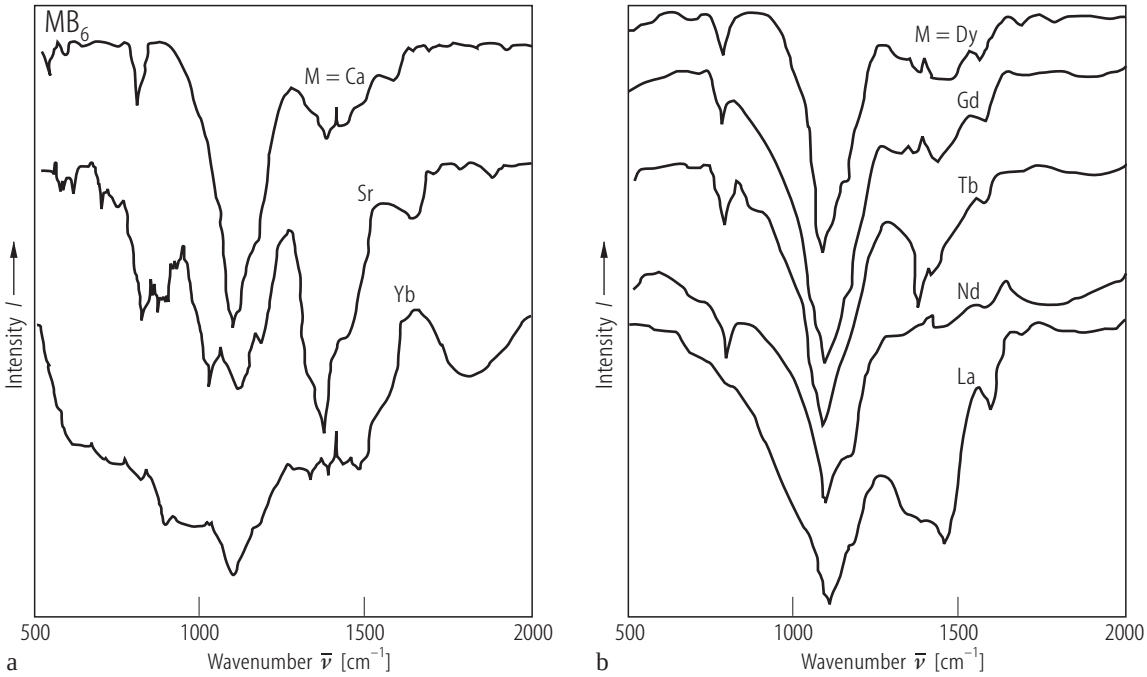

Fig. 10.

Metal hexaborides. Raman spectra, relative intensity vs. Raman shift for hexaborides with twofold and threefold ionized metal atoms [88T, 93Y].

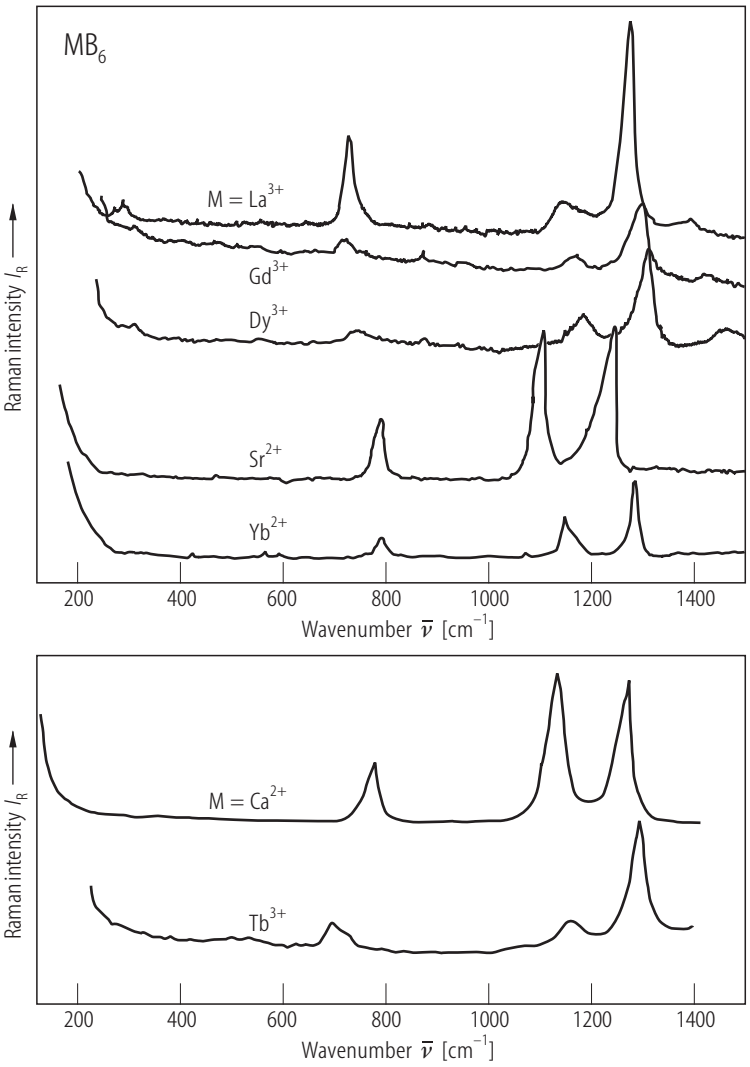

Fig. 11.

SrB_6. Calculated electronic band structure [97M].

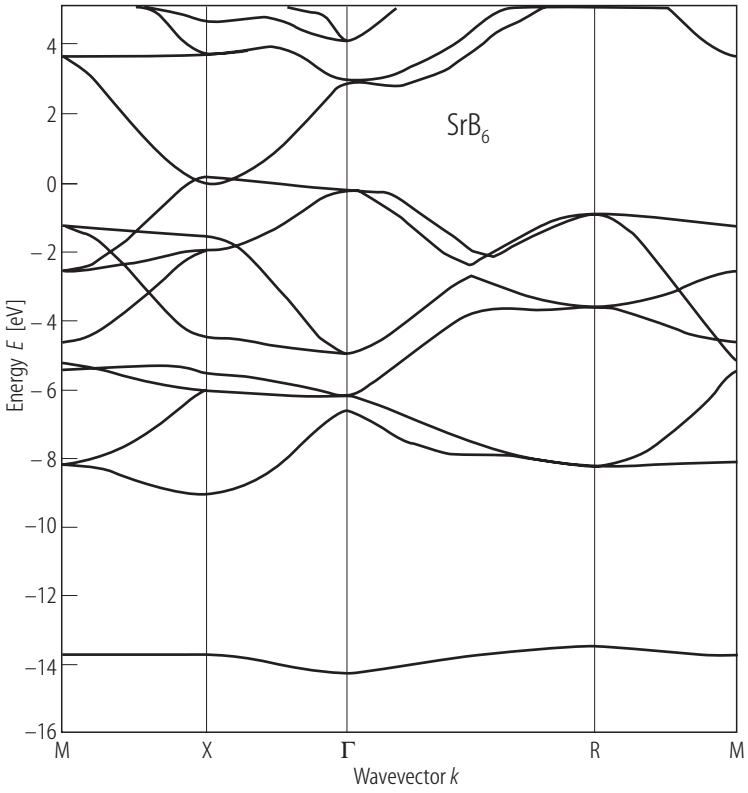

Fig. 12.

SrB_6. Calculated density of states. **(a)** Total DOS; **(b)** component DOS for B: dashed line, s states; solid line, p states; **(c)** component DOS for Sr: dashed line, s states; solid line, d states. Insert: DOS around E_F [97M].

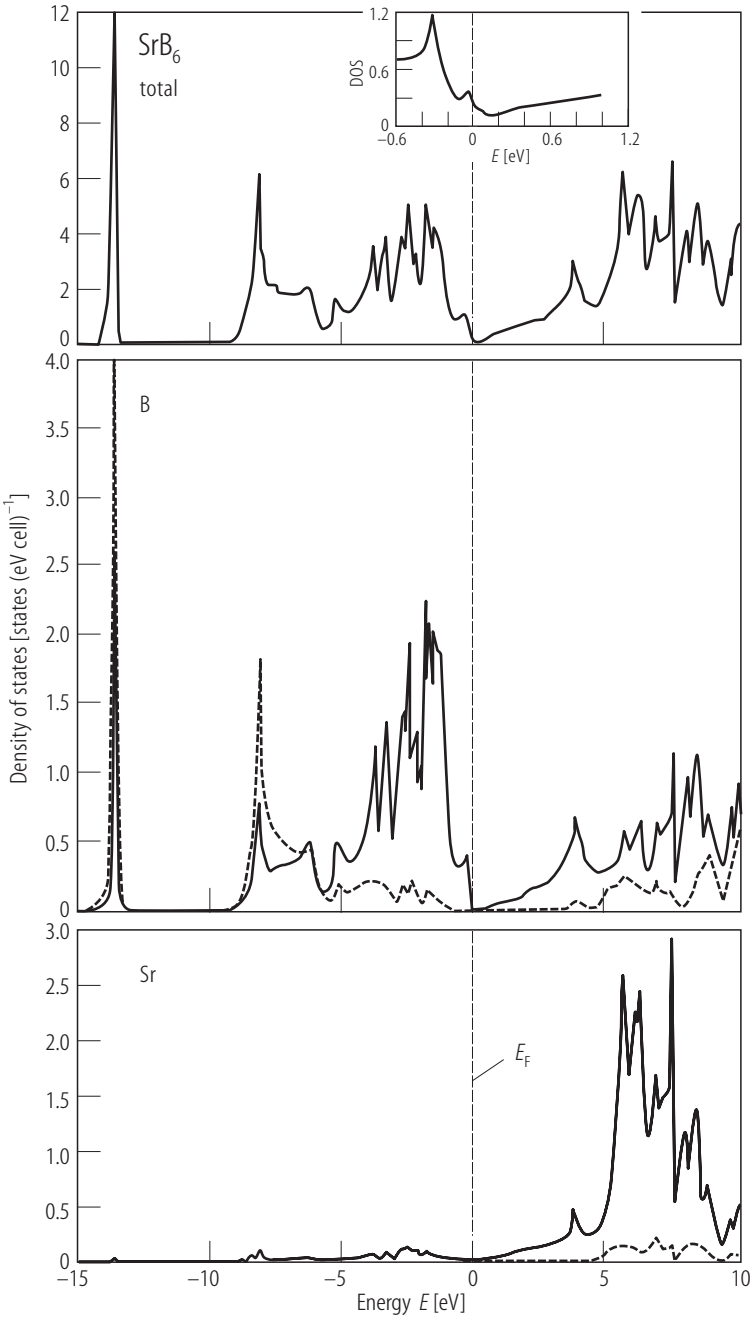

Fig. 13.

SrB_6. Variation of Raman spectra with the change of investigated particle within the same sample. Variation ranges: A_{1g}: 1190...1225; E_g: 1044...1078; F_{2g}: 738...770 cm^{-1} [93Y].